Article

Compact Single-Frequency MOPA Using a Silica Fiber Highly Doped with Yb^{3+}

Enkeleda Balliu [1,*], Magnus Engholm [1], Michel J. F. Digonnet [2], Riaan S. Coetzee [3], Gunnar Elgcrona [3] and Hans-Erik Nilsson [4]

[1] Department of Electronics Design, Mid Sweden University, Holmgatan 10, 851 70 Sundsvall, Sweden; Magnus.Engholm@miun.se
[2] Applied Physics Department, Stanford University, Stanford, CA 94305, USA
[3] Cobolt, Hübner Company, 171 54 Solna, Sweden; Riaan.Coetzee@cobolt.se (R.S.C.); gunnar.elgcrona@cobolt.se (G.E.)
[4] Faculty of Science, Technology and Media, Mid Sweden University, Holmgatan 10, 851 70 Sundsvall, Sweden; hans-erik.nilsson@miun.se
* Correspondence: enkeleda.balliu@miun.se

Abstract: We report on a single-frequency fiber master oscillator power amplifier utilizing a polarization-maintaining step-index fiber with an Al/Ce/F core-glass composition doped with a very high Yb concentration (0.25 at.%). This design made it possible to use a very short fiber (~1 m) and to coil it in a tight radius (4 cm in the amplifier, while 2 cm gave similarly negligible bending loss) so that the packaged system is one of the most compact reported to date (~0.6 L). The use of a short fiber increased the threshold for stimulated Brillouin scattering well above 100 W while maintaining near-ideal beam quality. The fiber was pumped with a diode-pumped solid-state laser and cooled passively by spooling it on a grooved aluminum mandrel. The amplifier produced a strongly linearly polarized output at 1064 nm in the fundamental mode ($M^2 \leq 1.2$) with a 150 kHz linewidth and a power of 81.5 W for 107 W of launched pump power. No deleterious effects from the elevated thermal load were observed. The residual photodarkening loss resulting from the high Yb concentration, found to be small (~0.7 dB/m inferred at 1064 nm) with accelerated aging, reduced the output power by only ~20% after 150 h of operation.

Keywords: Yb-doped fibers; single frequency; fiber amplifier; photodarkening; compact fiber amplifier

1. Introduction

The development of high-power single-frequency Yb-doped laser sources has been stimulated by both scientific interest and industrial applications. High-power lasers with a narrow linewidth (sub-kHz to 100 kHz), very low relative intensity noise (RIN) [1], and high beam quality are required in applications such as high-precision resonant fiber sensors [2] and nonlinear optical conversion [3]. The required output powers are up to hundreds of watts in the mid-infrared regime and tens of watts in the visible and UV regimes, ideally in a compact package form. A technique that has been extensively studied to meet these requirements is the fiber master oscillator power amplifier (MOPA). It is composed of a seed laser followed by one or more amplification stages utilizing rare-earth-doped fibers. Power scaling in a single-frequency fiber MOPA is often limited by the onset of stimulated Brillouin scattering (SBS) in the gain fiber. SBS arises from the interaction of acoustic phonons with the propagating signal wave, which is converted into a frequency-shifted, backward-propagating wave [4]. Several effective techniques have been developed to suppress SBS. Some of these techniques rely on modifying the modal or spectral properties of the seed laser [5–8]. In spite of their effectiveness, most of these techniques require additional components that increase size, cost, and complexity,

and degrade reliability. Other techniques mitigate SBS by modifying the gain fiber. These modifications include utilizing a special gain fiber, for example with a large mode area (LMA) [9,10], a high Yb concentration [11], or a taper [12]. SBS has also been pushed back by applying a temperature [13,14] or strain gradient [15] to the gain fiber. Achieving output powers in excess of 100 W requires more than one mitigation technique [9,16]. These techniques are particularly essential when amplifying a signal with a linewidth narrower than the SBS gain bandwidth (~23 MHz in silica [17]), in which case the SBS threshold is low.

Of the various classes of high-power Yb-doped fiber MOPAs, this paper is concerned strictly with single-frequency amplifiers with an output of 50–100 W with emphasis on minimizing size, cost, and complexity, even at the cost of a somewhat reduced output power. To this end, we consider only single-stage MOPAs, which in general utilize the fewest number of components and have the smallest footprint, and MOPAs that implement no SBS-suppression technique, for the same reasons. The highest output power reported for this class of amplifiers is 115 W [18]. It was achieved by bidirectional pumping and applying a temperature gradient to suppress SBS. A similar power was reported using a chirally-coupled-core (3C) fiber [16], although a large coiling diameter (0.3 m) was required. Intrinsic temperature gradient induced by backward pumping was used to achieve outputs of 20.1 W [19] and 108 W [9]. These devices required long fibers (~9 m), although the MOPA in [9] had a small bend diameter of 10 cm in spite of using an LMA fiber.

To meet the joint objectives of SBS suppression and compactness, this work explores the use of a conventional step-index fiber with a high Yb doping level. Optimizing the design of such a fiber requires careful selection of several parameters that have opposing effects on performance. First, for SBS suppression, the Yb concentration must be as high as possible to minimize the fiber length. Second, the fiber must be single-mode or near-single-mode to ensure a diffraction-limited output. Third, to reduce the system's footprint, the fiber must be wound in a tight coil while inducing minimal bending loss to the fundamental mode. This implies that LMA fibers are not preferred, since they typically (though not always [9]) require a large bend radius. It also implies that the core mode must not be too weakly guided. Finally, for SBS suppression, the fiber must carry as large a mode as possible while remaining near single-mode. The high Yb doping requires a high Al and/or P concentration to mitigate photodarkening (PD), which worsens with Yb concentration and limits the output power [20]. In turn, a high Al content raises the core index, which tends to increase the number of modes, while P reduces the cross-sections and gain [21]. Finally, the use of a short fiber with a high pump absorption raises the issue of potentially detrimental thermal loading.

This work is the first to investigate a fiber MOPA with an Al/Ce/F core-glass composition and a very high Yb concentration (0.25 at.% Yb). The focus was on experimentally determining the maximum obtainable power in light of the presence of residual photodarkening loss related to the high Yb concentration. Despite the practical challenges of manufacturing a glass of this composition that meets all requirements, the reported amplifier exhibits very good characteristics. It utilizes a 1-m gain fiber coiled on a passively cooled spool of small diameter (8 cm) and seeded with a diode-pumped solid-state laser. It produced a strongly linearly polarized output at 1064 nm in a clean mode with a linewidth of 150 kHz and a maximum output power of ~81.5 W for 107 W of pump power in a package slightly larger than half a liter. For comparison, the 130-W laser head of the Azurlight system [22] and the PreciLasers [23] have volumes of ~13 L and ~6.2 L, respectively. The amplifier reported here is 10 to 20 times more compact, which is made possible by the short active fiber and fewer optical components. There was no sign of SBS and no deleterious effects from the thermal load. The residual photodarkening loss was small enough that the output power decreased by only 20% over 150 h of operation.

2. Materials and Methods

The custom Yb-doped fiber tested as an amplifier (fiber I in Table 1) struck a compromise between the conflicting requirements mentioned above. It was highly doped with 0.25 at.% Yb ($1.65 \times 10^{+26}$ Yb/m^3). It had a comparatively large NA (0.082), a 15-μm core diameter, and it carried two modes at the signal (1064 nm). No bending loss was observed down to a bend diameter of 4 cm. Two commercial fibers (see Table 1) were tested for comparison. They were selected because their Yb concentrations, though significantly lower, rank among the highest for quality commercial fibers and because their cores are sufficiently small to provide a stable fundamental output mode. Their measured cladding absorption at 976 nm is ~3 times lower than fiber I. For all three fibers, the inner cladding diameter was either 125 μm or 130 μm. The fiber lengths in the amplifiers were selected to achieve a small-signal pump absorption of 20 dB to strike a balance between increasing the SBS threshold (shorter fiber) and increasing the pump absorption and output power (longer fiber).

Table 1. Parameter values of the single-frequency fiber MOPAs.

Fiber	Cladding/Core Absorption at 976 nm	Core/Cladding Diameter	Core NA	Number of Core Modes	Fiber Length
I	~19.2/1300 dB/m	15/125 μm	0.082	2	1.05 m
II	~6.5/1015 dB/m	10/125 μm	0.080	1	2.83 m
III	~5.7/428 dB/m	15/130 μm	0.080	2	3.28 m

A high Yb concentration has the significant downside of increasing PD. PD manifests itself as an absorption loss at visible wavelengths with a tail extending to the 1-μm region, where it causes harmful attenuation of the pump and signal. This loss increases with increasing Yb concentration and Yb inversion [24]. The most successful PD mitigation techniques include co-doping the core glass with P [21,25] or Ce [21,26]. These elements also raise the core index. This effect is corrected by adding index-lowering co-dopants such as F or B, or by using a pedestal index profile [26]. Al_2O_3 is also routinely used to increase the solubility of Yb_2O_3 in the core glass, hence limiting concentration quenching. Two common glass compositions are therefore Yb/Al/P [20,21] and Yb/Al/Ce/F [27]. Our experimental investigations show that they both successfully mitigate PD while offering single-mode operation for Yb concentrations below ~0.15 at.%. For higher Yb levels, however, achieving single-mode operation is much more difficult due to the challenges associated with incorporating high fluorine doping levels. Adding more fluorine than in fiber I is possible, but it can result in a non-uniform mix of Yb, Al, and Ce concentrations (and refractive index) along the preform.

To determine the optimum glass composition for our custom fiber, the suppression of PD was quantified by measuring the core loss induced by PD in three test fibers with different Ce/Yb ratios, numbered I, IV, and V (Table 2). They were custom aluminosilicate fibers with different concentrations of Ce but similar Yb concentration. A typical experimental setup [28] for accelerated PD evaluation was used. A short fiber (20–40 mm) was core-pumped with 450 mW of 976 nm light to ensure a nearly uniform Yb inversion of ~50%. Figure 1a plots the loss measured over time. After 20 h the PD loss was ~600 dB/m in the fiber with no Ce, ~200 dB/m in the fiber with a Ce/Yb ratio of 0.32, and ~33 dB/m for a ratio of 0.85. Thus, a prominent suppression of PD is observed even at a low Ce/Yb ratio of 0.32. However, it also shows that the Ce/Yb ratio should approach or exceed unity to achieve extremely low PD levels, in broad agreement with [21]. In light of this result, fiber I was selected for our amplifier work. Its Ce/Yb ratio of 0.32 was deemed sufficient because the inversion in the amplifier was much lower: 14.1% at maximum pump power. Its small-signal core absorption at 976-nm was ~1300 dB/m, which is ~1.3 times higher than in fiber II and ~3 times higher than in fiber III (see Table 1). Its cladding absorption was also higher due to its higher core-to-cladding areas ratio (as well as higher Yb concentration). Fiber IV was not selected, despite its higher resistance to photodarkening, because it had a

lower Yb concentration, which would negatively impact compactness, and a higher core NA, which makes single-mode operation more difficult.

Table 2. Composition of test fibers (at.%).

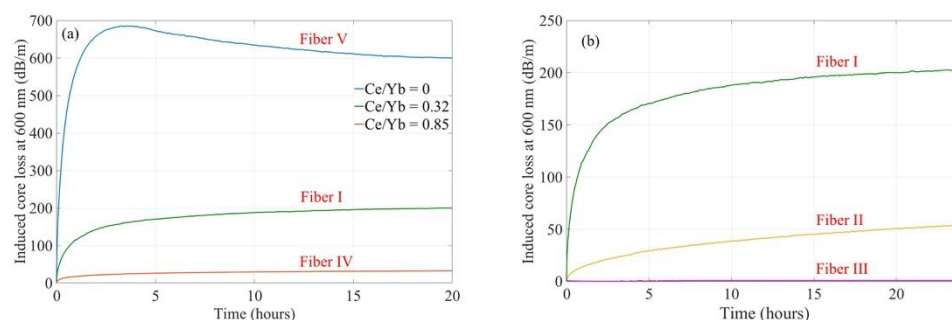| Fiber	[Yb]	[Al]	[Ce]	[F]
I	0.25	0.70	0.08	1.1
IV	0.20	1.1	0.17	0.78
V	0.27	0.92	0	1.07

Figure 1. Core loss induced at 600 nm by photo-darkening measured (**a**) in three fibers with similar Yb concentrations but different Ce/Yb ratios (see Table 2), and (**b**) in the three fibers used in the fiber amplifiers.

The results of the accelerated aging are plotted in Figure 1. After 24 h, the core loss in the custom fiber I was nearly 4 times higher than in fiber II, while fiber III had a much smaller loss. The PD loss, which decreases rapidly with increasing wavelength, was estimated using [24] to be ~80 times lower at 1064 nm (~2–2.5 dB/m), and ~40 times lower at 976 nm (~5 dB/m). At the lower inversion used in the amplifier (14.1%), it was expected to be ~3.5 times lower still [29], or only ~0.6–0.7 dB/m at 1064 nm and ~1.4 dB/m (5 dB/m divided by 3.5) at 976 nm. However, the loss at 976 nm has a much lower impact on long-term power stability than the loss at 1064 nm because the pump is mostly guided in the cladding, which does not suffer from photodarkening.

The MOPA architecture is shown in Figure 2. The seed laser was a 1064-nm diode-pumped solid-state laser (Cobolt, a Hübner Group Company). It is based on a unidirectional ring-cavity design and can generate up to 3 W of linearly polarized output power with a polarization extinction ratio (PER) greater than 30 dB. The laser 3-dB linewidth, measured with a delayed self-heterodyne interferometer, was ~150 kHz. It was kept below 2.5 W not to exceed the power rating of the tap coupler. Its output was free-space coupled into a PM isolator with a coupling efficiency of ~85% for the 10-μm-core fiber, and 90% for the 15-μm-core fibers. A 1% polarization-maintaining (PM) tap coupler was spliced to the output fiber of the isolator to monitor the backward-propagating power returning from the amplifier. The 99% output fiber pigtail of the tap coupler was spliced to the PM Yb-doped fiber. The active fiber was coiled around an aluminum spool with a diameter of 8 cm, so that the two 15-μm-core fibers, which are multimode at 1064 nm, carry a single mode. The spool had a U groove for better conductive cooling, and the fiber was covered by copper tape for increased heat conduction. The Yb-doped fiber was cladding-pumped in the backward direction by two wavelength-stabilized fiber-coupled 976 nm pump diode modules with a maximum power of 60 W each. The pump modules were spliced to the 105/125 μm pump fibers of a high-power pump/signal (2+1)×1 PM combiner. Finally, the output end of the Yb-doped fiber was spliced to the output fiber of the combiner. The pump power reflected by the combiner and the unwanted signal power in the cladding were efficiently removed by a 20-cm single-cladding passive fiber with the same core size as the gain fiber. Its output end was cleaved at 8° to avoid reflections. A high-index gel was

placed at the pump-output end of the Yb-doped fiber (see Figure 2) to remove unabsorbed pump light from the cladding.
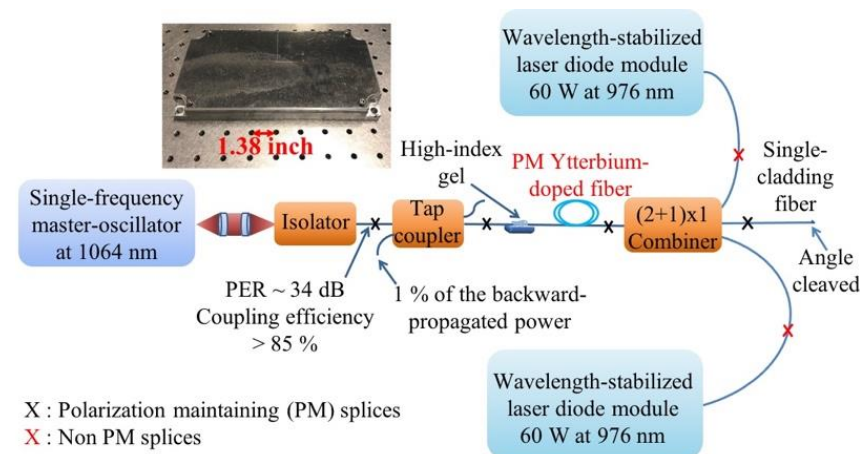

Figure 2. Schematic of the double-clad Yb-doped MOPA fiber amplifier. Photograph shows the packaged amplifier.

3. Results and Discussion

Figure 3 presents the output power and backward SBS power measured against pump power for all three amplifiers with gain-fiber lengths of 1.05 m (I), 2.83 m (II), and 3.28 m (III). The lengths of the combiner's fiber pigtails were shortened as much as possible (~48 cm) to increase the SBS threshold. The launched seed power was ~2 W. No limit due to SBS was observed for fiber I up to the maximum pump power of 107.4 W, providing an output power as high as 81.5 W (green filled lozenges in Figure 3). Significantly lower output power was reached with fiber II, with an observed SBS threshold of 33 W, while an SBS-limited output power of 58 W was reached with the larger (15 μm) core fiber III. A much shorter gain fiber would be required to increase the SBS threshold further using fiber III, but this would reduce the slope efficiency considerably. The slope efficiency with fiber I was 75%, only slightly lower than with fiber III (78%).
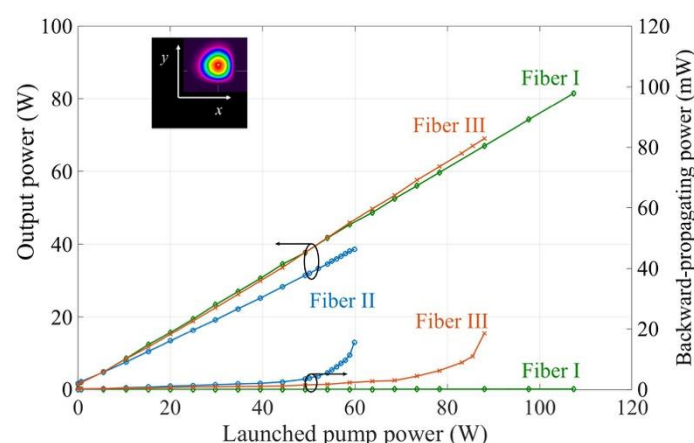

Figure 3. Output power (left axis) and backward SFS output power (right axis) measured versus launched pump power for fiber amplifiers utilizing 1.05 m of fiber I, 2.83 m of fiber II, or 3.28 m of fiber III. Inset is an image of the output mode profile, measured at 52 W of output power.

The temperature distribution along the fiber, measured with an infrared camera, was fairly uniform along the fiber, primarily because of the use of backward pumping. The temperature was slightly higher near the pump-input end of the fiber, as expected. At outputs above 50 W, the measured temperature of fiber I was 40 °C due to the higher

thermal load associated with the fiber's high absorption. The output power was limited by the available pump power, not by thermal effects. In routine runs, as mentioned earlier, the fiber was covered with copper tape, which improved heat dissipation, so the actual fiber temperature was lower than 40 °C. The IR camera could unfortunately not measure the actual temperature due to the presence of the tape. Although it was not the main focus of this work, handling this increased fiber temperature at higher power levels (~80 W) is a straightforward engineering task that should not introduce undue complications. A small amount of forced-air cooling, or passive cooling with fins, would easily reduce the temperature further. Finally, we note that at the highest output power, the power stability was better than 1%, indicating that the thermal load was insufficient to cause undue power fluctuations.

For beam-quality measurements, the output beam of the amplifier was refocused with a lens to a large spot size (to avoid damage), and the beam profile was measured versus distance from the focal plane with a high-damage-threshold Nanoscan 2s pyro-electric camera from Ophir. The camera recorded a 2D image of the mode and calculated the mode's transverse dimension along the horizontal (x) and vertical (y) axis. These data points were fitted to the well-known expression of the diffraction of a Gaussian beam in air. A 2D image of the output mode is shown in the inset of Figure 3. The mode energy is confined to the fundamental mode, with a small asymmetry (the x-axis in the image is related to the spatial orientation of the cleave plane). The fits performed by the camera yielded an M^2 value of 1.39 in x and 1.09 in y. These values are likely to be overestimated because the position of the camera was measured by hand, which increased the error in the measured diffraction curve. In these measurements, the fiber was straight, so the asymmetry cannot be attributed to a combination of fiber bending and high thermal load. The fiber output facet was cleaved at an angle, which also explains the slight asymmetry in the mode profile and in M^2.

The signal-to-noise ratio (SNR) of the MOPA amplifier using fiber I was measured with an OSA. The SNR was 61 dB when the seed power was 1.5 W, and 68 dB for 2.5 W. It was limited by amplified spontaneous emission (ASE), which decreased as the seed power was increased. The PER was measured with a half-wave plate and a polarizing beam splitter. It varied with pump power between ~19 dB and ~35 dB, with a mean value of ~27 dB.

To quantify the impact of PD on the amplifier's output power, the latter was recorded continuously over 150 h at a nominally constant pump power, starting from an output power of 3 W. This test was carried out at lower power than the maximum output power (80 W) to avoid residual thermal effects. Performing this test at higher power would have introduced thermal fluctuations in the fiber amplifier output power, which would have partly masked the photodarkening effect that the test aims to characterize, thereby rendering the outcome of the test inconclusive. To validate this decision from the standpoint of photodarkening, we estimated the values of the photodarkening loss at these two powers. Simulations using a validated commercial code showed that, at 3 W, the inversion along the fiber was approximately uniform with an average value of 12.2%. In comparison, at maximum power (80 W), it had a similar distribution with an average only slightly higher (14.1%). Since the equilibrium PD loss is proportional to inversion [30], the loss at the 3-W power used in long-term measurements and at 80 W are very close to each other, and the PD behavior is expected to be similar at both powers. Based on the core loss inferred from PD measurements at 600 nm in fiber I (200 dB for an inversion of 50%, see Figure 1b), the proportionality factor is 4 dB/m per percent of inversion. Therefore, the influence on the photodarkening loss at 600 nm of the 1.9% higher inversion (at 80 W compared to 3 W) is 7.6 dB/m. As mentioned earlier, this loss value is 80–100 times lower at 1064 nm, or only 0.076–0.095 dB/m, and ~40 times lower at 976 nm, or 0.19 dB/m, which, as pointed out earlier, is less important than the loss at 1064 nm. The difference in photodarkening losses at 3 W and 80 W is clearly negligible. Furthermore, at increased temperature the PD loss actually decreases [31]. Therefore, this second effect at least partially cancels the first effect,

which is very weak in the first place. Based on the foregoing, a low-power test is adequate to characterize the power degradation at any power.

The result (Figure 4) indicates that the power degraded minimally, decreasing asymptotically to 2.4 W (20%) over 150 h. Experimental observations suggest that the increase in fiber temperature at higher power reduces the equilibrium loss due to PD [31]. Therefore, at higher power the fractional power drop may be even lower. We expect that at the maximum pump power of 107 W, after degradation, the MOPA would output ~80% of 81.5 W, or ~65 W. Our numerical prediction of the SBS power threshold shows that this concept can be scaled to output powers up to 100 W for an available pump power of 130 W.
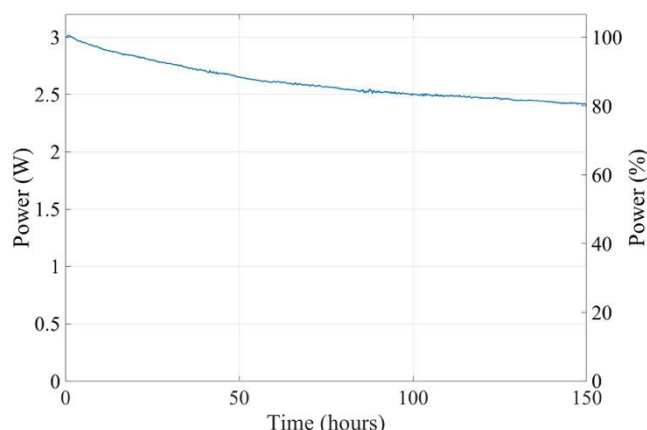

Figure 4. Measured output power of the MOPA using fiber I showing a slow decrease over time as a result of residual photodarkening loss.

4. Conclusions

We have reported a single-frequency polarization-maintaining fiber MOPA utilizing a highly Yb-doped fiber with a relatively large NA. This combination efficiently suppressed SBS while allowing the fiber to be coiled on a very small mandrel (2 cm radius), thus producing a compact packaged device. Its performance shows that the silica fiber technology is now at a stage where fibers with sufficiently high Yb concentrations can be fabricated for compact, simple MOPA amplifiers outputting tens of watts and offering a good trade-off between SBS suppression, beam quality, thermal load, and photodarkening. Future work should focus on further improving the core-glass composition to further reduce the reduction in power due to the residual photodarkening loss. Possible avenues include increasing the Ce concentration and offsetting the related increase in core index by increasing the fluorine concentration or with a pedestal index profile.

References

1. Buikema, A.; Jose, F.; Augst, S.J.; Fritschel, P.; Mavalvala, N. Narrow-linewidth fiber amplifier for gravitational-wave detectors. *Opt. Lett.* **2019**, *44*, 3833–3836. [CrossRef]
2. Skolianos, G.; Arora, A.; Bernier, M.; Digonnet, M.J.F. Photonics sensing at the thermodynamic limit. *Opt. Lett.* **2017**, *42*, 2018–2021. [CrossRef] [PubMed]
3. Sinha, S.; Hum, D.S.; Urbanek, K.E.; Lee, Y.-W.; Digonnet, M.J.F.; Fejer, M.M.; Byer, R.L. Room-temperature stable generation of 19 Watts of single-frequency 532-nm radiation in a periodically poled lithium tantalate crystal. *J. Light. Technol.* **2008**, *26*, 3866–3871. [CrossRef]
4. Boyd, R.W. *Nonlinear Optics*, 3rd ed.; Elsevier: San Diego, CA, USA, 2008; pp. 429–471.
5. Platonov, N.; Yagodkin, R.; Cruz, J.D.L.; Yusim, A.; Gapontsev, V. Up to 2.5 kW on non-PM fiber and 2.0 kW linear polarized on pm fiber narrow linewidth CW diffraction-limited fiber amplifiers in all-fiber format. *Proc. SPIE* **2018**, *10512*, 105120E.
6. Beier, F.; Hupel, C.; Kuhn, S.; Hein, S.; Nold, J.; Proske, F.; Sattler, B.; Liem, A.; Jauregui, C.; Limpert, J.; et al. Single mode 4.3 kW output power from a diode-pumped Yb-doped fiber amplifier. *Opt. Express* **2017**, *25*, 14892–14899. [CrossRef] [PubMed]
7. Goodno, G.D.; Rothenberg, J.E. Suppression of stimulated Brillouin scattering in kilowatt fiber amplifier using nonlinear spectral compression. In *Laser Congress 2018 (ASSL)*; Optica Publishing Group: Washington, DC, USA, 2018.
8. Zeringue, C.; Vergien, C.; Dajani, I. Pump-limited, 203 W, single-frequency monolithic fiber amplifier based on laser gain competition. *Opt. Lett.* **2011**, *36*, 618–620. [CrossRef] [PubMed]
9. Liem, A.; Limpert, J.; Zellmer, H.; Tünnermann, A. 100-W single-frequency master-oscillator fiber power amplifier. *Opt. Lett.* **2003**, *28*, 1537–1539. [CrossRef] [PubMed]
10. Robin, C.; Dajani, I.; Pulford, B. Modal instability-suppressing, single-frequency photonic crystal fiber amplifier with 811 W output power. *Opt. Lett.* **2014**, *39*, 666–669. [CrossRef]
11. Balliu, E.; Engholm, M.; Nilsson, H.-E. A compact, single-frequency, high-power, SBS-free, Yb-doped single- stage fiber amplifier. *Proc. SPIE* **2019**, *10896*, 1089618.
12. Shiraki, K.; Ohashi, M.; Taleda, M. Suppression of stimulated Brillouin scattering in a fiber by changing the core radius. *Electtron. Lett.* **1995**, *31*, 668–669. [CrossRef]
13. Theeg, T.; Sayinc, H.; Neumann, J.; Kracht, D. All-fiber counter-propagation pumped single frequency amplifier stage with 300-W output power. *IEEE Photonics Technol. Lett.* **2012**, *24*, 1864–1867. [CrossRef]
14. Kovalev, V.I.; Harrison, R.G. Suppression of stimulated Brillouin scattering in high-power single-frequency fiber amplifiers. *Opt. Lett.* **2006**, *31*, 161–163. [CrossRef] [PubMed]
15. Yoshizawa, N.; Imai, T. Stimulated Brillouin scattering suppression by means of applying strain distribution to fiber with cabling. *J. Light. Technol.* **1993**, *11*, 1518–1522. [CrossRef]
16. Hochheim, S.; Steinke, M.; Wessels, P.; de Varona, O.; Koponen, J.; Lowder, T.; Novotny, S.; Neumann, J.; Kracht, D. Single-frequency chirally coupled-core all-fiber amplifier with 100 W in a linearly polarized TEM00 mode. *Opt. Lett.* **2020**, *45*, 939–942. [CrossRef] [PubMed]
17. Agrawal, G. *Nonlinear Fiber Optics*, 5th ed.; Elsevier: Waltham, MA, USA, 2013; pp. 355–384.
18. Hildebrandt, M.; Büsche, S.; Weßels, P.; Frede, M.; Kracht, D. Brillouin scattering spectra in high-power single frequency ytterbium doped fiber amplifiers. *Opt. Express* **2008**, *16*, 15970–15979. [CrossRef]
19. Höfer, S.; Liem, A.; Limpert, J.; Zellmer, H.; Tünnermann, A.; Unger, S.; Jetschke, S.; Müller, H.R.; Freitag, I. Single-frequency master-oscillator fiber power amplifier system emitting 20 W of power. *Opt. Lett.* **2001**, *26*, 1326–1328. [CrossRef] [PubMed]
20. Jauregui, C.; Stutzki, F.; Tünnermann, A.; Limpert, J. Thermal analysis of Yb-doped high-power fiber amplifiers with Al:P co-doped cores. *Opt. Express* **2018**, *26*, 7614–7624. [CrossRef] [PubMed]
21. Jetschke, S.; Unger, S.; Schwuchow, A.; Leich, M.; Kirchhof, J. Efficient Yb laser fibers with low photodarkening by optimization of the core composition. *Opt. Express* **2008**, *16*, 15540–15545. [CrossRef]
22. Azurlight Systems. Available online: https://azurlight-systems.com/ (accessed on 14 September 2021).
23. PreciLasers. Available online: https://precilasers.com/en/ (accessed on 14 September 2021).
24. Koponen, J.J.; Söderlund, M.J.; Hoffman, H.J.; Tammela, S.K.T. Measuring photodarkening from single-mode ytterbium doped silica fibers. *Opt. Express* **2006**, *14*, 11539–11544. [CrossRef]
25. Engholm, M.; Norin, L. Preventing photodarkening in ytterbium-doped high power fiber lasers; correlation to the UV-transparency of the core glass. *Opt. Express* **2008**, *16*, 1260–1268. [CrossRef]
26. Engholm, M.; Jelger, P.; Laurell, F.; Norin, L. Improved photodarkening resistivity in ytterbium-doped fiber lasers by cerium cooping. *Opt. Lett.* **2009**, *34*, 1285–1287. [CrossRef]
27. Li, Y.; Liu, S.; Zhan, H.; Peng, K.; Sun, S.; Jiang, J.; Wang, X.; Ni, L.; Jiang, L.; Wang, J.; et al. Fiber design and fabrication of Yb/Ce codoped aluminosilicate laser fiber with high laser stability. *IEEE Photon. J.* **2018**, *10*, 1502908. [CrossRef]
28. Koponen, J.; Söderlund, M.; Tammela, S.; Kliner, D.; Koplow, J. Photodarkening measurements in LMA fibers. *Proc. SPIE* **2007**, *6453*, 64531E.
29. Koponen, J.; Söderlund, M.; Hoffman, H.J.; Kliner, D.A.V.; Koplow, J.P.; Hotoleanu, M. Photodarkening rate in Yb-doped silica fibers. *Appl. Opt.* **2008**, *47*, 1247–1256. [CrossRef] [PubMed]

30. Jetschke, S.; Unger, S.; Röpke, U.; Kirchhof, J. Photodarkening in Yb doped fibers: Experimental evidence of equilibrium states depending on the pump power. *Opt. Express* **2007**, *15*, 14838–14843. [CrossRef]
31. Leich, M.; Jetschke, S.; Unger, S.; Kirchhof, J. Temperature influence on the photodarkening kinetics in Yb-doped silica fibers. *J. Opt. Soc. Am. B* **2011**, *28*, 65–68. [CrossRef]